http://dx.doi.org/10.5935/0103-5053.20140010

J. Braz. Chem. Soc., Vol. 25, No. 4, 629-638, 2014.
Printed in Brazil - ©2014 Sociedade Brasileira de Química
0103 - 5053 $6.00+0.00

Article

Experimental and NMR Theoretical Methodology Applied to Geometric Analysis of the Bioactive Clerodane *trans*-Dehydrocrotonin

Breno Almeida Soares,[a] Caio Lima Firme,*[,a] Maria Aparecida Medeiros Maciel,[a,b] Carlos R. Kaiser,[c] Eduardo Schilling[d] and Adailton J. Bortoluzzi[d]

[a]*Universidade Federal do Rio Grande do Norte, Instituto de Química, Campus Lagoa Nova, 59072-970 Natal-RN, Brazil*

[b]*Programa de Pós-graduação em Biotecnologia, Universidade Potiguar Laureate International Universities, Campus Salgado Filho, 59075-000 Natal-RN, Brazil*

[c]*Universidade Federal do Rio de Janeiro, Instituto de Química, Ilha do Fundão, 21941-909 Rio de Janeiro-RJ, Brazil*

[d]*Universidade Federal de Santa Catarina, Departamento de Química, Campus Universitário Trindade, 88040-900 Florianópolis-SC, Brazil*

trans-Desidrocrotonina (*t*-DCTN), um bioditerpeno do tipo 19-*nor*-clerodano isolado de *Croton cajucara* Benth, representa um dos clerodanos da atualidade com maiores índices de investigações científicas. Neste trabalho, uma nova abordagem unindo dados de difração de raios X, dados de ressonância magnética nuclear (NMR) e dados teóricos foi aplicada para a completa caracterização da *t*-DCTN. Para tanto, a geometria de *t*-DCTN foi reavaliada por difração de raios X e NMR de ^{1}H e ^{13}C e foi comparada com os dados teóricos obtidos por B3LYP/6-311G++(d,p). A subsequente avaliação dos valores teóricos e experimentais de deslocamentos químicos de NMR e constantes de acoplamento spin-spin apresentou correlações muito boas entre propriedades magnéticas teóricas e experimentais. Adicionalmente, os índices de deslocalização entre átomos de hidrogênio, δ(H,H'), correlacionaram bem com os dados experimentais e calculados de constante de acoplamento. Uma análise topológica complementar utilizando a teoria quântica de átomos em moléculas (QTAIM) mostrou interações intramoleculares para *t*-DCTN.

trans-Dehydrocrotonin (*t*-DCTN) a bioactive 19-*nor*-diterpenoid clerodane type isolated from *Croton cajucara* Benth, is one of the most investigated clerodane in the current literature. In this work, a new approach joining X-ray diffraction data, nuclear magnetic resonance (NMR) data and theoretical calculations was applied to the thorough characterization of *t*-DCTN. For that, the geometry of *t*-DCTN was reevaluated by X-ray diffraction as well as ^{1}H and ^{13}C NMR data, whose geometrical parameters where compared to those obtained from B3LYP/6-311G++(d,p) level of theory. From the evaluation of both calculated and experimental values of ^{1}H and ^{13}C NMR chemical shifts and spin-spin coupling constants, it was found very good correlations between theoretical and experimental magnetic properties of *t*-DCTN. Additionally, the delocalization indexes between hydrogen atoms correlated accurately with theoretical and experimental spin-spin coupling constants. An additional topological analysis from quantum theory of atoms in molecules (QTAIM) showed intramolecular interactions for *t*-DCTN.

Keywords: *Croton cajucara*, *trans*-dehydrocrotonin, NMR, DFT calculations, QTAIM, X-ray crystallography

*e-mail: firme.caio@gmail.com, caiofirme@quimica.ufrn.br

Introduction

The clerodane group of diterpenes includes more than 800 isolated compounds and a significant number showed to have biological activity such as antimicrobial,[1] psychotropic,[2] antiulcer[3] and antitumor.[4] Actually, the 19-*nor*-clerodane *trans*-dehydrocrotonin (*t*-DCTN), a furan clerodane skeleton type diterpene (Figure 1), is one of the most important bioactive clerodane reported in the current literature. This natural compound isolated from *Croton cajucara* Benth (Euphorbiaceae), a widely grown tree in the Amazonian region of Northern Brazil, became an important target for pre-clinical researches. In fact, pharmacological studies examining *t*-DCTN confirmed its anti-inflammatory, analgesic, antitumor, antiulcer, hypolipidemic and cardioprotective effect.[5,6] *t*-DCTN has also been shown to have antimutagenic activity[5-7] and did not induce clastogenic, anticlastogenic, apoptotic and cytotoxic activities.[8]

In general, a complete characterization of natural terpenoids compounds requires a large amount of work, in which 1D and 2D-nuclear magnetic resonance (NMR) techniques can be combined with X-ray diffraction analysis. Since 1976, when Ferguson and Marsh reported the first crystallographic analysis of a diterpenoid type clerodane molecule,[9] a plenty of reports arises describing clerodane molecules by crystallographic analysis in combination with NMR techniques. Owing to the complexity of clerodane structural molecule, the X-ray diffraction analysis is an important tool for a reliable and complete structural analysis of a new natural or semi-synthetic organic compound. In this context, the use of theoretical quantum chemistry methods becomes a complementary tool for structural analysis of organic compounds.[3,10-26]

The NMR spectral data of a new compound provide an useful information for its molecular identity and geometry. In fact, NMR parameters such as chemical shifts and spin-spin coupling constants (SSCC), as well as theoretical calculations and ^{1}H spectrum simulations give support for the total characterization of complex molecules. Regarding the SSCC parameter, it plays an important role on the conformational analysis and elucidation of several types of molecules,[27-31] mainly when it is correlated with theoretical SSCC.[32-43]

Most of the theoretical descriptions of spin spin coupling constants follows the Ramsey and Purcell interpretation[44] and Ramsey formulation.[45] In this method, the coupling constants are calculated by adding four different terms: (1) diamagnetic spin orbit (DSO) as well as (2) the paramagnetic spin orbit (PSO), which represent the interactions of the magnetic field of the nuclei mediated by the electron orbital motion, (3) the Fermi contact (FC), which is also a response property reflecting the interaction between the electron spin magnetic moment close to the nucleus and the magnetic field at the nucleus, and (4) the spin dipole (SD), which describes the interactions between the nuclear magnetic moments as mediated by the electronic spin angular moment. For an accurate quantum chemical description of SSCCs all the terms cited above must be considered.[46-49] In addition, the delocalization index between two hydrogen atoms, $\delta(H,H')$, can also be used in the theoretical analysis of the SSCCs.[50]

The quantum theory of atoms in molecules (QTAIM)[51] is based on an observable, the electron density, and it has been

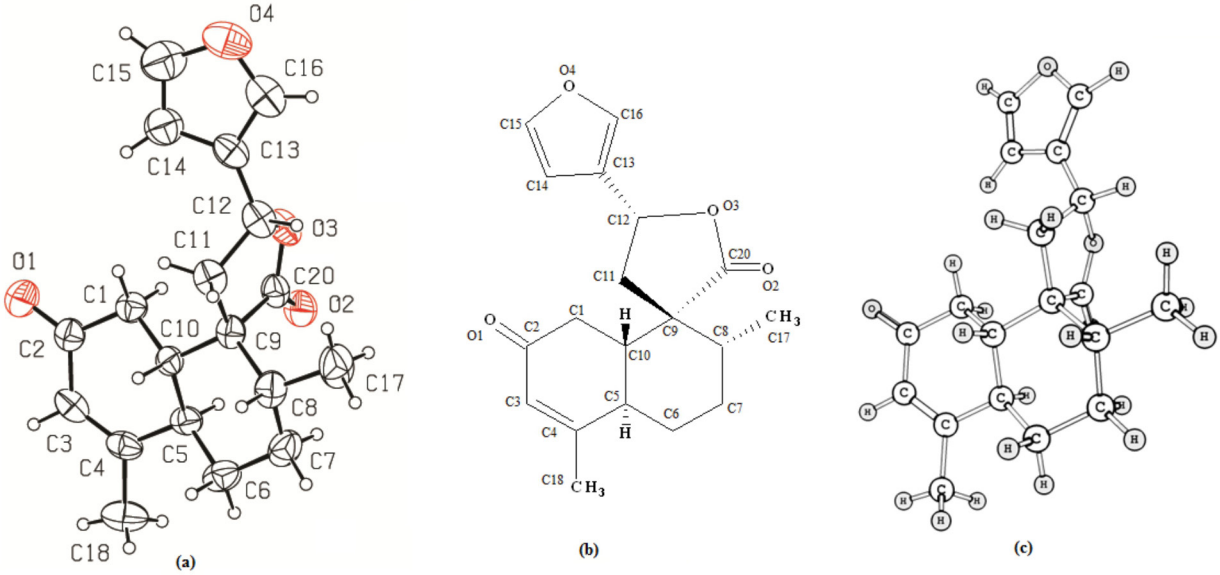

Figure 1. (a) Crystallographic structure, (b) skeleton formula and (c) optimized structure from B3LYP/6-311G++(d,p) level of theory of the clerodane *t*-DCTN.

used for several experimental applications, for example, the estimate of the intensity of infrared (IR) spectrum[52,53] and magnetic susceptibility,[54] as well as the calculation of topological information from X-ray diffraction data[55] and the linear correlation between delocalization index δ(H,H′) and proton-proton coupling constants.[56-58] The linear correlation between delocalization index and fluorine fluorine coupling constants was also described.[59]

Unambiguous NMR assignments for *t*-DCTN and its stereochemistry determination were previously reported using a powerful NMR equipment (600 MHz for ^{1}H), 2D-NMR experiments, AM1 calculations and ^{1}H NMR spectrum simulations.[60] In the present work, we have performed X-ray diffraction of *t*-DCTN and many theoretical calculations using B3LYP. The geometric skeleton of *t*-DCTN was re-examined by means of several correlations involving experimental and theoretical data in order to provide additional structural information such as bond length and dihedral angles measurements which are extensively used in the conformational analysis of biomolecules applied to its pharmacological responses.[3,12,24] Correlations between theoretical results and corresponding experimental data plus topological analysis from QTAIM are herein discussed.

Experimental

Material and methods

Plant material was collected in Jacundá City located at Pará State (Amazonian region, Brazil), and identified by Nelson A. Rosa.[5] A voucher specimen (no. 247) has been stored at the Herbarium of the Museu Paraense Emílio Goeldi (Belém, PA, Brazil). The isolation of *t*-DCTN was performed according to the literature[5] and its recrystallization (from a mixture of hexane:ether 7:3) yielded suitable crystal for X-ray diffraction. The assignments for structure elucidation were previously determined from ^{1}H (600 MHz) and ^{13}C (150 MHz) NMR spectroscopy.[60]

Single crystal X-ray diffraction

The crystal data were measured on an Enraf-Nonius CAD4 diffractometer using graphite monochromated Mo-K_α radiation (λ = 0.71069 Å) at room temperature. A colorless crystal with dimensions of 0.40 × 0.33 × 0.30 mm was isolated from a homogeneous crystalline sample of *t*-DCTN. Unit-cell parameters were determined from centering of 25 reflections in the θ angle ranging from 4.92 to 12.03° and refined by the least-squares method according to standard procedure.[61] Intensities were collected using the ω-2θ scan technique. All diffracted intensities were corrected by Lorentz and polarization effects. The structure was solved by direct methods and was refined by the full-matrix least-squares method using SIR97 and SHELXL97.[62,63] All non-hydrogen atoms were refined with anisotropic displacement parameters. Hydrogen atoms were placed at idealized positions using standard geometric criteria. The PLATON program[64] was used to generate the picture of the molecular structure. Further relevant crystallographic data are summarized in Table 1.

Table 1. Crystal data and structure refinement for *t*-DCTN

Empirical formula	$C_{19}H_{22}O_4$
Formula weight	314.37
Temperature / K	293(2)
Wavelength / Å	0.71073
Crystal system	Orthorhombic
Space group	$P2_12_12_1$
a / Å	7.3869(8)
b / Å	13.8966(13)
c / Å	16.018(3)
Volume / Å^3	1644.3(4)
Z	4
ρ / (g cm^3)	1.270
μ / mm^{-1}	0.088
F(000)	672
Crystal size	0.40 × 0.33 × 0.30 mm^3
Theta range for data collection	1.94 to 27.97°
Index ranges	-9 ≤ h ≤ 0. -18 ≤ k ≤ 0. -21 ≤ l ≤ 0
Reflections collected / unique	2184 / 2184 [R(int) = 0.0000]
Completeness to theta = 27.97°	96.2 %
Absorption correction	None
Refinement method	Full-matrix least-squares on F^2
Data / restraints / parameters	2184 / 0 / 208
Goodness-of-fit on F^2	0.982
Final R indices [I > 2σ(I)]	R1 = 0.0502; wR2 = 0.1076
R indices (all data)	R1 = 0.1753; wR2 = 0.1386
Largest diff. peak and hole / (e Å^{-3})	0.170 and –0.105

Crystallographic data (atomic coordinates and equivalent isotropic displacement parameters, calculated hydrogen atom parameters, anisotropic thermal parameters and bond lengths and angles) have been deposited at the Cambridge Crystallographic Data Center (deposition number CCDC 276648). Copies of this information may be obtained free of charge from: CCDC, 12 Union Road, Cambridge, CB2 1EZ, UK (Fax: +44-1223-336-033; e-mail: deposit@ccdc.cam.ac.uk or http://www.ccdc.cam.ac.uk).

Computational details

The geometry of the studied species was optimized using standard techniques.[65] Vibrational analysis of *t*-DCTN optimized geometry was carried out to determine whether it was a true minimum or a transition state. No imaginary frequency was obtained confirming that a minimum was found in the potential energy surface. The calculations were performed at B3LYP/6-311G++(d,p)[66-71] using GAUSSIAN 09 package.[72] From the Kohn-Sham orbitals of *t*-DCTN optimized structure, the electron density was obtained and then used for the calculation of *t*-DCTN topological data by means of the AIM2000 software.[73]

Results and Discussion

The DFT procedures for computing proton-proton coupling constants and/or chemical shifts of unknown structures or targets from synthetic studies, have been extensively reported.[32-38] In this work, aiming to describe the most stable conformational status of *t*-DCTN (Figure 1) more thoroughly, we have examined the combined set of X-ray data, NMR spectra and computational calculations using B3LYP/6-311G++(d,p) level of theory. A single crystal X-ray diffraction was undertaken in order to re-examine the asymmetric centers (C5, C8, C9, C10 and C12) of *t*-DCTN. The PLATON perspective drawing (Figure 1a) is in agreement with the geometric configuration supported by NMR spectra of *t*-DCTN. The theoretical analysis of geometric and magnetic properties of *t*-DCTN gives additional support for its experimental characterization since it confirms the structure of the most stable conformer of *t*-DCTN.

Figure 1 shows the crystallographic structure of *t*-DCTN (Figure 1a), the corresponding skeleton formula (Figure 1b) and its optimized structure obtained from B3LYP/6-311G++(d,p) (Figure 1c). In the perspective drawing (Figure 1a and 1c), the conformation of the decalin system chair is distorted due to $\Delta^{3,4}$ double bond (located at C3 and C4 in the so-called ring A) and also the spiro-lactone at C9 (in the so-called ring B).

Geometrical data available in the Supplementary Information indicate that the hydrogen atoms at C10 and C5 positions are on the opposite side of A/B decalin system, assuming *trans* configuration (Table S1 from Supplementary Information). In addition, the bond lengths and angles are as expected for a *trans* geometry for *t*-DCTN.

The existence of the spiro arrangement in lactone moiety can be noticed by the fact that C9 is shared by the lactone group itself and also by ring B of decalin system. The α,β-unsaturated carbonyl group located in C2, C3, C4 and O1 atoms of decalin ring A could be observed revealing similar bond lengths of 3-(4-chloro-benzene-sulfonamido)-5-methyl-cyclo-hex-2-en-1-one, whose geometric and topological parameters were described by Jackson and co-workers.[74] The C=O, C=C and C–C bond lengths of 3-(4-chloro-benzene-sulfonamido)-5-methyl-cyclo-hex-2-en-1-one (1.251, 1.356 and 1.437 Å, respectively) are comparable to those corresponding bonds in ring A of *t*-DCTN (1.215, 1.325 and 1.449 Å, respectively).

The minimum in the potential energy surface of *t*-DCTN was obtained by B3LYP/6-311G++(d,p) level of theory whose geometrical parameters were compared with those from X-ray diffraction (Table S1 from Supplementary Information). The theoretical and experimental parameters for *t*-DCTN are very similar, except for some angle values from furan and lactone moieties. The O3–C12–C11, C15–C14–C13 and C13–C16–C14 angles have nearly two degrees of discrepancy when comparing theoretical and experimental results (See Supplementary Information). The root mean square deviation (RMSD) of *t*-DCTN bond lengths and bond angles was calculated in order to measure the accuracy of theoretical results in comparison with X-ray data. The RMSD values are 0.0153 and 0.9333 for bond lengths and bond angles, respectively. These values show the precision of the chosen level of theory for geometric calculations of *t*-DCTN and also indicate the relatively smaller precision of calculated bond angles with respect to experimental values.

As a consequence of agreement between experimental and theoretical results, Figure 1a (PLATON thermal ellipsoids plots) and Figure 1c (an optimized structure) indicate similar nuclear configuration for *t*-DCTN. Both stereo views showed a visual similarity in arrangements of the decalin and lactone moieties, as well as for furan ring, which is out of plane for both representations.

Theoretical magnetic properties (chemical shifts and SSCC) of *t*-DCTN were obtained from B3LYP/6-311G++(d,p) level of theory and compared with corresponding experimental values (See Supplementary Information).

Aiming to reinforce the discussion on the absolute configuration of *t*-DCTN, correlations between the experimental NMR data[60] and theoretical NMR chemical shifts of *t*-DCTN are presented in Figures 2a (^{1}H NMR chemical shifts, in ppm) and 2b (^{13}C NMR chemical shifts, in ppm). Thereby we found very good linear correlations between the experimental and theoretical NMR chemical shifts as indicated by their corresponding coefficient of determinations. The agreement between experimental (both X-ray and NMR data) and the corresponding theoretical data from our applied computational protocol, indicate

that B3LYP/6-311G++(d,p) level of theory suffices for the analysis of magnetic and geometric properties of the evaluated clerodane *t*-DCTN.

The vicinal or long range coupling constants of *t*-DCTN were calculated from the gauge-independent atomic orbital (GIAO) method including the four contributing terms (FC, PSO, DSO, SD)[46] at the B3LYP/6-311G++(d,p) level of theory. The B3LYP/GIAO method provides accurate coupling constant values in many systems, being most of them related to rigid structure and/or aromatic molecular systems.[37-40]

A reasonably good correlation between calculated and experimental coupling constants was obtained (Figure 3), except for those values involving hydrogen atoms 8 and 17, whose differences between experimental and theoretical values were larger than three ppm. Therefore, the B3LYP/6-311G++(d,p)/GIAO method, including the four contributing terms (FC, PSO, DSO, SD), suffices to describe magnetic properties of low symmetry and flexible structures similar to *t*-DCTN.

The delocalization index from QTAIM is the quantity of shared electrons in an atomic pair, bonded or non-bonded,

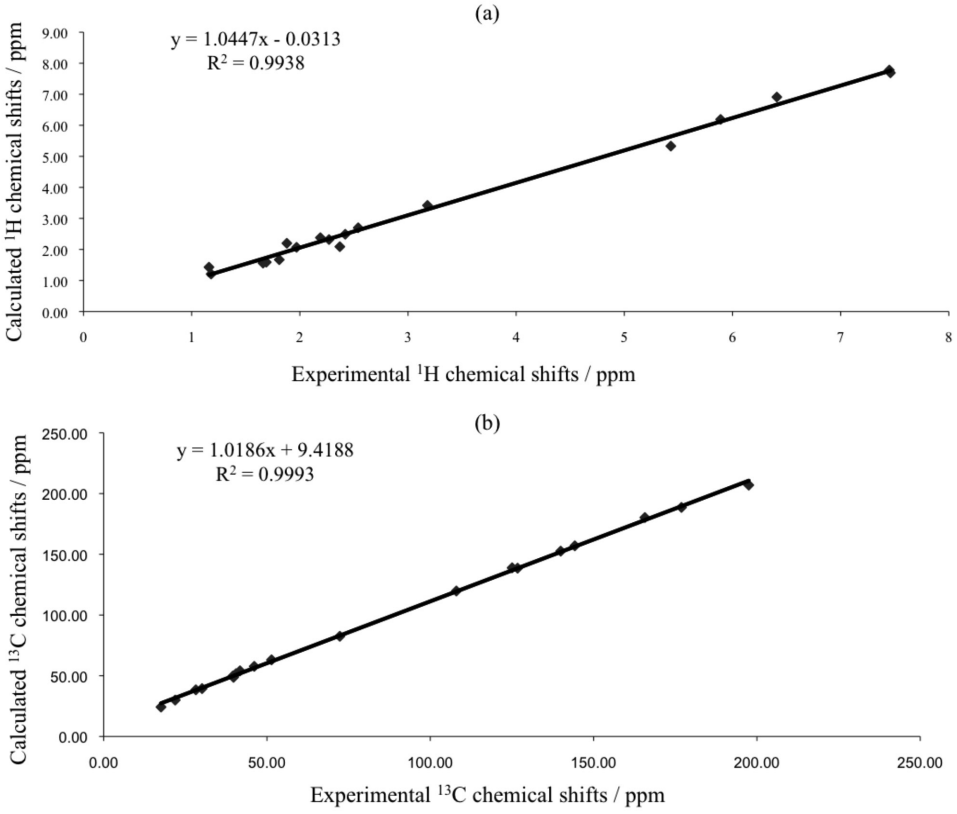

Figure 2. (a) Plot of experimental *vs.* calculated (B3LYP/6-311G++(d,p)) ^{1}H NMR chemical shifts and (b) plot of experimental *vs.* theoretical ^{13}C NMR chemical shifts for *t*-DCTN.

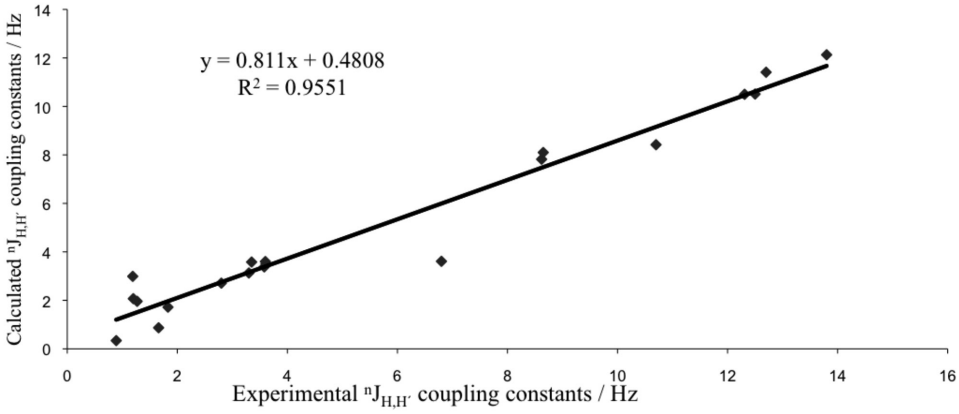

Figure 3. Plot of experimental *vs.* calculated (B3LYP/6-311G++(d,p)) ^{1}H vicinal or long range NMR spin-spin coupling constants [^{n}J (H,H′)] for *t*-DCTN.

and it has been used to establish a relation with coupling constants of many molecular systems.[56] There are excellent correlations observed in literature[37,56-58] between delocalization index of vicinal or long range hydrogen atoms δ(H,H') and corresponding experimental coupling constants. Additionaly, fluorine fluorine coupling constants also showed satisfactory correlation with delocalization index data for aromatic systems.[59]

Figures 4a and 4b shows the plots of experimental and theoretical coupling constants versus corresponding delocalization index of vicinal or long range hydrogen atoms of *t*-DCTN, respectively. Both of them give a reasonably good coefficient of determination, meaning that the amount of shared charge density between long or vicinal hydrogen atoms is related with the magnitude of the corresponding coupling constant, i.e., a relation between electronic and magnetic properties of *t*-DCTN is established in Figure 4. According to Gutowsky and collaborators,[75] the spin-spin coupling arises from second-order interaction between the nuclear magnetic moments and some magnetic field internal to the molecule through electrons along chemical bonding. The results from Figure 4 suggest that the influence of weak electron interaction, through field effect, between the interacting nuclei plays some role in long range or vicinal spin-spin coupling as well, which concords with J-couplings in hydrogen bonds.[76,77]

Aiming at the investigation of possible intramolecular interactions in *t*-DCTN, we also carried out its topological analysis based on the gradient of the charge density distribution. Figure 5 shows the molecular graph of *t*-DCTN which contains critical points of the charge density and bond paths. Critical point is a mathematical point of a determined function, whose gradients, with respect to their coordinates, are zero. The topology of charge density may have four types of critical points: the nuclear attractor critical point (where it is located an atomic nucleus), the bond critical point (a critical point between two linking atoms), the ring critical point (a critical point within a ring) and the cage critical point (a critical point inside a molecular cage). The bond path is an atomic interaction line linking two nuclear critical points (or atomic basins) and one bond critical point between them. It corresponds to the maximum charge density compared to vicinal transversal region.[51]

Figure 5 shows the molecular graph of the *t*-DCTN which has five bond critical points associated with

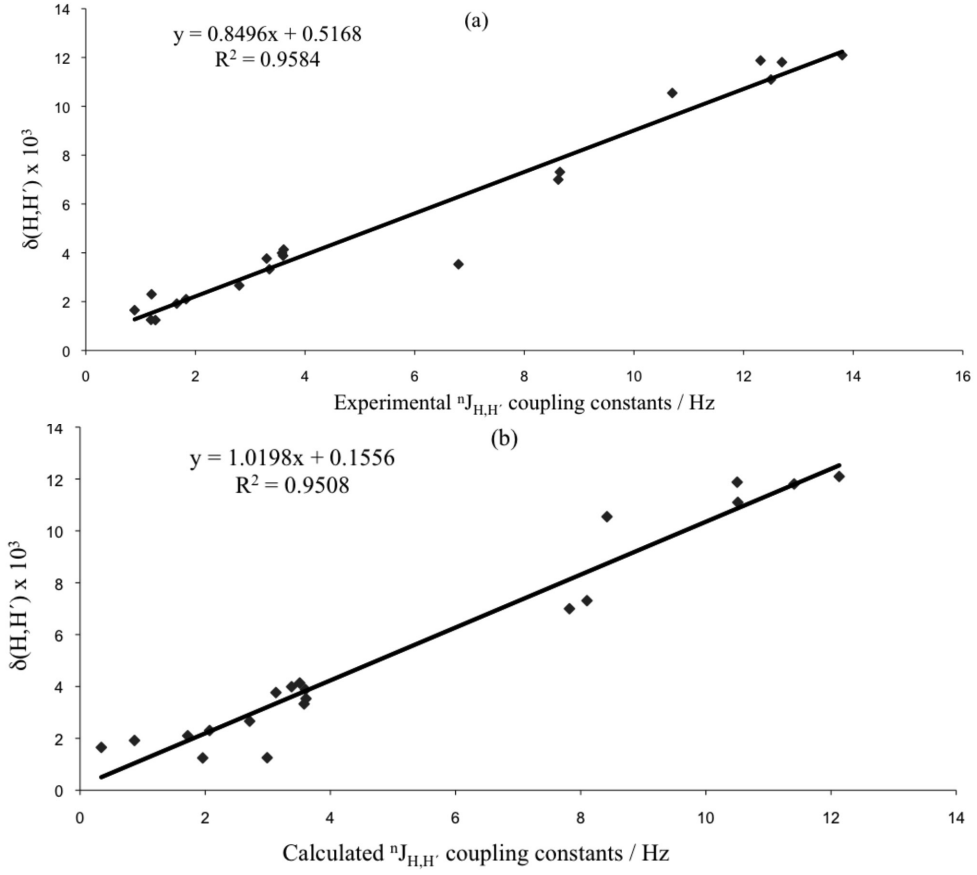

Figure 4. (a) Plot of experimental spin-spin coupling constants of vicinal or long range protons [J^n (H,H′)] *vs.* corresponding delocalization index values δ(H,H′); (b) plot of calculated spin-spin coupling constants (B3LYP/6-311G++(d,p)) *vs.* corresponding delocalization index δ(H,H′) for *t*-DCTN.

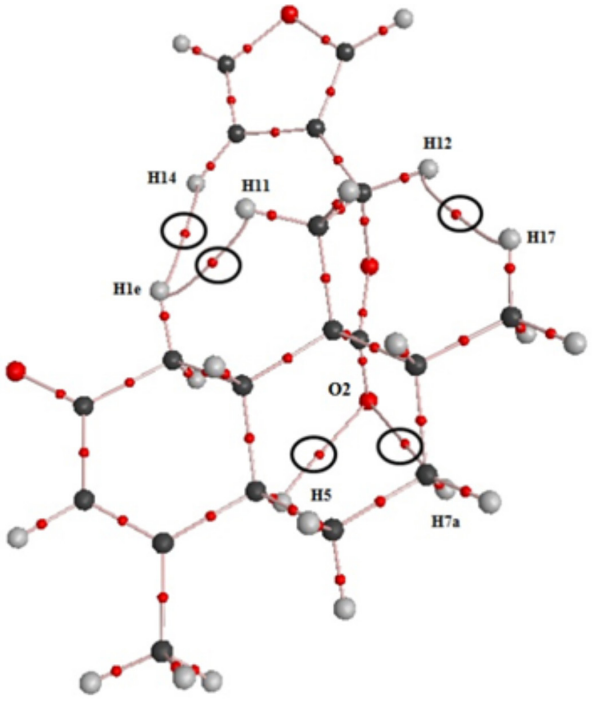

Figure 5. Molecular graph for *t*-DCTN indicating the bond paths analyzed in Table 2.

intramolecular closed-shell interactions, where three out of them are hydrogen-hydrogen bonds (Table 2).

An important applicability of QTAIM is to quantify and qualify bonded interactions based on five topological parameters obtained at the analyzed bond critical point:[78-81] (1) the value of the charge density of the critical point (ρ_b); (2) the value and the sign of the Laplacian ($\nabla^2\rho$) of the charge density; (3) the ratio $|\lambda_1|/\lambda_3$, where λ_1 and λ_3 are eigenvalues of Hessian matrix of the charge density; (4) the ratio G_b / ρ_b, where G_b is the kinetic energy density; and (5) the total energy density (H_b) at the bond critical point. In the case where $\nabla^2\rho > 0$, ρ_b is relatively low ($\rho_b < 6 \times 10^{-2}$ a.u.), the ratio $|\lambda_1|/\lambda_3 < 1$, the ratio $G_b / \rho_b > 1$ or close to 1, and H_b has a positive value, close to zero, the chemical interaction is defined as closed shell interaction and it corresponds, for example, to hydrogen bond, ionic bond and van der Waals interactions.[78-81] Table 2 shows these five topological data for all intramolecular bonded interaction in *t*-DCTN (Figure 5) which are certainly related to the highest stability of *t*-DCTN found in its NMR and X-ray data.

All values in Table 2 are in agreement with the topological characterization of closed shell interaction for the five interatomic interactions.[78-81] The values of G_b/ρ_b in Table 2 are in the same range to that found in closed shell interactions in metallocenes, involving metal atom and π ligand carbon atom.[82] The most stable conformer of *t*-DCTN presents five intramolecular interactions: three H-H bonds, linking hydrogen atoms from decalin system to hydrogen atoms from spiro-lactone and furan rings, and two (C)O--H(C) bonded interactions linking the lactone carbonyl oxygen to two axial hydrogen atoms from decalin ring. It is demonstrated in literature that H–H bonding contributes as a stabilizing factor to the energy of a chemical system.[81,83] Matta and co-workers have investigated intramolecular H–H bonding in several compounds showing its stabilizing effect whose values of the five topological parameters listed in Table 2 were similar to the H–H bonds in *t*-DCTN.

Regarding the (C)O--H(C) bonded interactions we compared the charge density of bond critical points and Laplacian of the charge density between (C)O--H(C) bonded interactions and the corresponding values from hydrogen bonds (O--HO) of substituted malonaldehyde enols.[84] The charge density of (C)O--H(C) bonded interactions are nearly one-fifth of the averaged charge density value of hydrogen bonds of substituted malonaldehyde enols. On the other hand, according to less positive values of $\nabla^2\rho$ of the bond critical point related to (C)O--H(C) bonded interactions in *t*-DCTN, the corresponding distribution of the charge density is less dispersed in (C)O--H(C) bonded interactions in *t*-DCTN than that in hydrogen bonds of substituted malonaldehyde enols.[84]

Therefore, the sum of the charge density in the five intramolecular interactions in *t*-DCTN is nearly equivalent to the charge density of one hydrogen bond of malonaldehyde enol,[84] which shows the cooperative effect of the five weak intramolecular interactions in determining the most stable conformer of *t*-DCTN. Three intramolecular interactions (H–H bonds) are not influenced by polarity

Table 2. Values of the charge density of bond critical points (ρ_b), the corresponding Laplacian of the charge density ($\nabla^2\rho$), the ratio $|\lambda_1| / \lambda_3$, the ratio G_b / ρ_b, and the total energy density (H_b) of all intramolecular bonded interactions in *t*-DCTN

Interactions	$\rho_b \times 10^2$ / a.u.	$\nabla^2\rho$ / a.u.	$\lvert\lambda_1\rvert / \lambda_3$	G_b / ρ_b	$H_b \times 10^2$ / a.u.
H1e–H11	1.285	0.045	0.194	0.721	1.653
H1e–H14	0.384	0.012	0.175	0.632	0.487
H17–H12	0.771	0.026	0.162	0.705	0.971
O2–H7a	0.882	0.029	0.167	0.722	1.186
O2–H5	1.139	0.036	0.184	0.707	1.512

while it influences the other two interactions involving oxygen atom. Indeed, the most stable conformer of *t*-DCTN is the one obtained by means of NMR and X-ray whose experimental values are in very good agreement with the corresponding theoretical data. Then, our theoretical calculations reinforced the characterization of the most stable conformer and also enabled a clear understanding of the electronic structure of *t*-DCTN.

Currently, there is a number of *Croton cajucara* Benth researches devoted to its chemical, biochemical, pharmacological and more recently potential advantages of molecular incorporation into drug delivery systems, specifically DCTN-load studies.[85-88] In fact, concerning to the biotechnological advanced context, our recent work reported to *trans*-dehydrocrotonin cover its encapsulation in liposomes with a significant enhancement of the antitumor activity of this 19-*nor*-clerodane-type diterpene.[85] Since the stability of *t*-DCTN loaded in different biological formulations had been investigated aiming its pharmacologic improvement, this present work attracts significant importance on physicochemical characteristics of this compound to be applied in the advancement of this drug uses in therapy. For that, in this present work, a new approach joining two different methodologies, previously applied to organic compounds, has been developed and validated for the thorough characterization of some complex organic compounds such as the natural bioactive *t*-DCTN.

Conclusions

The crystallographic and theoretical data are in agreement with the previously detailed NMR analysis and characterization of the structure of *t*-DCTN. Experimental and theoretical geometric parameters present nearly negligible discrepancies, indicating that B3LYP/6-311G++(d,p) is a satisfactory level of theory for the calculation of the optimized geometry of complex molecules such as *t*-DCTN. Those results confirmed the stereochemistry of the decaline and lactone units and a hindered rotation around the C12–C13 bond in *t*-DCTN.

There are very good correlations involving experimental and theoretical magnetic properties (NMR nuclear shielding and spin-spin coupling constants), indicating that: (1) the B3LYP/6-311G++(d,p)/GIAO method is satisfactory for the calculation of NMR nuclear shielding and; (2) the B3LYP/311G++(d,p)/GIAO method is satisfactory for the calculation of spin-spin coupling constants.

The values of QTAIM delocalization indexes involving vicinal or long range hydrogen atoms correlate well with both corresponding theoretical and experimental spin-spin coupling constants of *t*-DCTN, indicating that the amount of charge density between each proton pair (being vicinal or not) is directly proportional to the spin-spin coupling constant.

From the topological analysis of *t*-DCTN there are five intramolecular bonded interactions in *t*-DCTN (three out of them being hydrogen-hydrogen bonds) which possibly influence in the optimal nuclear configuration and the geometric structure of *t*-DCTN.

A new approach joining two different methodologies, previously applied to organic compounds, has been developed and validated in this work for the thorough characterization of complex organic compounds.

Supplementary Information

Selected bond length and bond angles from X-ray diffraction and B3LYP method, experimental and theoretical ^{1}H and ^{13}C NMR chemical shifts, experimental and theoretical NMR spin-spin coupled constants, Z-matrix and crystallographic data for *t*-DCTN. This material is available free of charge at http://jbcs.sbq.org.br as PDF file.

Acknowledgments

The authors are grateful to FAPERN (Fundação de Amparo à Pesquisa do Estado do Rio Grande do Norte), CAPES (Coordenação de Aperfeiçoamento de Pessoal de Nível Superior) and CNPq (Conselho Nacional de Desenvolvimento Científico e Tecnológico) for financial support.

References

1. Murthy, M. M.; Subramanyam, M.; Bindu, M. H.; Annapurna, J.; *Fitoterapia* **2005**, *76*, 336.
2. Shirota, O.; Nagamatsu, K.; Sekita, S.; *J. Nat. Prod*. **2006**, *69*, 1782.
3. Brasil, D. S. B.; Alves, C. N.; Guilhon, G. M. S. P.; Muller, A. H.; Secco, R. S.; Peris, G.; Llusar, R.; *Int. J. Quan. Chem*. **2008**, *108*, 2564.
4. Ravikumar, Y. S.; Mahadevan, K. M.; Manjunatha, H.; Satyanarayana, N. D.; *Phytomedicine* **2010**, *17*, 513.
5. Maciel, M. A. M.; Pinto, A. C.; Arruda, A. C.; Pamplona, S. G.; Vanderlinde, F. A.; Lapa, A. J.; Echevarria, A.; Grynberg, N. F.; Cólus, I. M. S.; Farias, R. A. F.; Costa, A. M. L.; Rao, V. S. N.; *J. Ethnopharmacol.* **2000**, *70*, 41.
6. Costa, M. P.; Magalhães, N. S. S.; Gomes, F. E. S.; Maciel, M. A. M.; *Braz. J. Pharmacog.* **2007**, *17*, 275.
7. Âgner, A. R.; Maciel, M. A. M.; Pinto, A. C.; Pamplona, S. G.; Cólus, I. M.; *Teratogen. Carcin. Mut.* **1999**, *19*, 377.

8. Poersch, A.; Santos, F. V.; Maciel, M. A. M.; Câmara, J. K. P.; Dantas, T. N. C.; Cólus, I. M. S.; *Mutat. Res.* **2007**, *629*, 14.
9. Ferguson, G.; Marsh, W. C.; *Cryst. Struct. Commun*. **1976**, *5*, 35.
10. Herz, W.; Pilotti, A. M.; Soderholm, A. C.; Shuhama, I. K.; Vichnewski, W.; *J. Org. Chem*. **1977**, *42*, 3913.
11. Busygin, I.; Nieminen, V.; Taskinen, A.; Sinkkonen, J.; Toukoniitty, E.; Sillanpaa, R.; Murzin, D. Y.; Leino, R.; *J. Org. Chem*. **2008**, *73*, 6559.
12. Roslund, M. U.; Klika, K. D.; Lehtila, R. L.; Tahtinen, P.; Sillanpaa, R.; Leino, R.; *J. Org. Chem.* **2004**, *69*, 18.
13. Nishino, C.; Manabe, S.; Kazui, M.; Matsuzaki, T.; *Tetrahedron Lett.* **1984**, *25*, 2809.
14. Soriano-Garcia, M.; Toscano, R. A.; Esquivel, B.; Hernandez, M.; Rodriguez-Hahn, L.; *Acta Crystallogr., Sect. C: Cryst. Struct. Commun.* **1987**, *43*, 272.
15. Manriquez, V.; San-Martin, A.; Rovirosa, R.; von Schnering, H. G.; Peters, K. *Acta Crystallogr., Sect. C: Cryst. Struct. Commun.* **1990**, *46*, 1170.
16. Ning, X.; Zhi-Da, M.; Shou-Xun, Z.; Bing, W.; Qi-Tai, Z.; Pei, Z.; *Phytochemistry* **1991**, *30*, 1963.
17. Toscano, R. A.; Sanchez, A. A.; Esquivel, B.; Esquivel, O.; Rodriguez-Hahn, L.; *Acta Crystallogr., Sect. C: Cryst. Struct. Commun.* **1994**, *50*, 1794.
18. Huan-Ming, C.; Zhi-Da, M.; Iinuma, M.; Tanaka, T.; *Heterocycles* **1996**, *43*, 611.
19. Ye, D.; Shu-Lin, P.; Qiang, Z.; Xun, L.; Li-Sheng, D.; *Helv. Chim. Acta*. **2002**, *85*, 2547.
20. Januario, A. H.; Santos, S. L.; Marcussi, S.; Mazzi, M. V.; Pietro, R. C. R. L.; Sato, D. N.; Ellena, J.; Sampaio, S. V.; Franca, S. C.; Soares, A. M.; *Chem. Biol. Interact*. **2004**, *150*, 243.
21. Sathe, M.; Kaushik, M. P.; *Bioorg. Med. Chem. Lett*. **2010**, *20*, 1312.
22. Cantrell, C. L.; Klun, J. A.; Pridgeon, J.; Becnel, J.; Green III, S.; Fronczek, F. R.; *Chem. Biodivers*. **2009**, *6*, 447.
23. Liu, H.; Chou, G.; Guo, Y.; Ji, L.; Wang, J.; Wang, Z.; *Phytochemistry* **2010**, *71*, 1174.
24. Brasil, D. S. B.; Müller, A. H.; Guilhon, G. M. S. P.; Alves, C. N.; Peris, G.; Llusard, R.; Moline, V.; *J. Braz. Chem. Soc*. **2010**, *21*, 731.
25. Brasil, D. S. B.; Moreira, R. Y. O.; Müller, A. H.; Alves, C. N.; *Int. J. Quan. Chem*. **2006**, *106*, 2706.
26. Guo, P.; Li, Y.; Xu, J.; Liu, C.; Ma, Y.; Guo, Y.; *J. Nat. Prod*. **2011**, *74*, 1575.
27. Günther, H.; *NMR Spectroscopy: Basic Principles. Concepts and Applications in Chemistry*, 2nd ed.; John Wiley & Sons: New York, 1995.
28. Muller, N.; Pritchard, D. E.; *J. Chem. Phys.* **1959**, *31*, 768.
29. Karplus, M.; Anderson, D. H.; *J. Chem. Phys.* **1959**, *30*, 6.
30. Karplus, M.; *J. Chem. Phys.* **1959**, *30*, 11.
31. Karplus, M.; *J. Am. Chem. Soc.* **1963**, *85*, 2870.
32. Barone, V.; Peralta, J. E.; Contreras, R. H.; Snyder, J. P.; *J. Phys. Chem. A*. **2002**, *106*, 5607.
33. Pihlaja, K.; Tahtinen, P.; Klika, K. D.; Jokela, T.; Salakka, A.; Wahala, K.; *J. Org. Chem.* **2003**, *68*, 6864.
34. Bally, T.; Rablen, P. R.; *J. Org. Chem*. **2011**, *76*, 4818.
35. López-Vallejo, F.; Fragoso-Serrano, M.; Suárez-Ortiz, G. A.; Hernández-Rojas, A. C.; Cerda-García-Rojas, C. M.; Pereda-Miranda, R.; *J. Org. Chem.* **2011**, *76*, 6057.
36. Pu, J.; Huang, S.; Ren, J.; Xiao, W.; Li, L. M.; Li, R.; Li, L. B.; Liao, T.; Lou, L.; Zhu, H.; Sun, H.; *J. Nat. Prod*. **2007**, *70*, 1706.
37. Sánchez-Mendoza, E.; Hernández-Trujillo, J.; del Río-Portilla, F.; *J. Phys. Chem. A*. **2007**, *111*, 8264.
38. Del Bene, J. E.; Alkorta, I.; Elguero, J.; *J. Phys. Chem. A*. **2010**, *114*, 3713.
39. Alkorta, I.; Elguero, J.; Limbach, H.; Shenderovich, I. G.; Winkler, T.; *Magn. Reson. Chem*. **2009**, *47*, 585.
40. Czernek, J.; Lang, J.; Sklenář, V.; *J. Phys. Chem. A*. **2000**, *104*, 2788.
41. Gräfenstein, J.; Tuttle, T.; Cremer, D.; *Phys. Chem. Chem. Phys*. **2005**, *7*, 452.
42. Gräfenstein, J.; Kraka, E.; Cremer, D.; *J. Phys. Chem. A*. **2004,** *108*, 4520.
43. Bouř, P.; Raich, I.; Kaminský, J.; Hrabal, R.; Čejka, J.; Sychrovský, V.; *J. Phys. Chem. A*. **2004**, *108*, 6365.
44. Ramsey, N. F.; Purcell, E. M.; *Phys. Rev*. **1952**, *85*, 143.
45. Ramsey, N. F.; *Phys. Rev.* **1953**, *91*, 303.
46. Autschbach, J.; Le Guennic, B.; *J. Chem. Ed*. **2007**, *84*, 156.
47. Cremer, D.; Gräfenstein, J.; *Phys. Chem. Chem. Phys*. **2007**, *9*, 2791.
48. Helgaker, T.; Watson, M.; Handy, N. C.; *J. Chem. Phys*. **2000**, *113*, 9402.
49. Sychrovský, V.; Gräfenstein, J.; Cremer, D.; *J. Chem. Phys*. **2000**, *113*, 3530.
50. Bader, R. F. W.; Streitwieser, A.; Neuhaus, A.; Laidig, K. E.; Speers, P.; *J. Am. Chem. Soc*. **1996,** *118*, 4959.
51. Bader, R. F. W.; *Atoms in Molecules: A Quantum Theory*; Oxford University Press: Oxford, 1994.
52. Haiduke, R. L. A.; de Oliveira, A. E.; Bruns, R. E.; *J. Phys. Chem. A*. **2004**, *108*, 6788.
53. Haiduke, R. L. A.; Bruns, R. E.; *J. Phys. Chem. A*. **2005**, *109*, 2680.
54. Bader, R. F. W.; Keith, T. A.; *J. Chem. Phys.* **1993**, *99*, 3683.
55. Koritsanszky, T. S.; Coppens, P.; *Chem. Rev.* **2001**, *101*, 1583.
56. Matta, C. F.; Hernández-Trujillo, J.; Bader, R. F. W.; *J. Phys. Chem. A*. **2002**, *106*, 7369.
57. Mandado, M.; Blockhuys, F.; Alsenoy, C. V.; *Chem. Phys. Lett.* **2006**, *430*, 454.
58. Sánchez-Mendoza, E.; Hernández-Trujillo, J.; *Magn. Reson. Chem.* **2010**, *48*, 866.
59. Castillo, N.; Matta, C. F.; Boyd, R. J.; *J. Chem. Inf. Mod*. **2005**, *45*, 354.

60. Maciel, M. A. M.; Pinto, A. C.; Kaiser, C. R.; *Magn. Reson. Chem*. **2003**, *41*, 278.
61. Enraf-Nonius; *CAD-4 Software*; Enraf-Nonius, Delft, The Netherlands, 1989.
62. Altomare, A.; Burla, M. C.; Camalli, M.; Cascarano, G.; Giacovazzo, C.; Guagliard, A.; Moliterni, A. G. G.; Spagna, R.; *J. Appl. Crystallogr.* **1999**, *32*, 115.
63. Sheldrick, G.; *SHELXL-97 Program for Crystal Structure Refinement*; University of Göttingen, Germany, 1997.
64. Spek, A. L.; *Acta Crystallogr., Sect. D: Biol. Crystallogr.* **2009**, *65*, 148.
65. Fletcher, R.; *Practical Methods of Optimization*; Wiley: New York, 1980.
66. Becke, A. D.; *J. Chem. Phys*. **1993**, *98*, 5648.
67. Becke, A. D.; *J. Chem. Phys*. **1993,** *98*, 1372.
68. Dunning, J. T. H.; *J. Chem. Phys*. **1989**, *90*, 1007.
69. Head-Gordon, M.; Pople, J. A.; Frisch, M. J.; *Chem. Phys. Lett*. **1988**, *153*, 503.
70. Frisch, M. J.; Head-Gordon, M.; Pople, J. A.; *Chem. Phys. Lett*. **1990**, *166*, 281.
71. Frisch, M. J.; Head-Gordon, M.; Pople, J. A.; *Chem. Phys*. Lett. **1990**, *166*, 275.
72. Frisch, M. J.; Trucks, G. W.; Schlegel, H. B.; Scuseria, G. E.; Robb, M. A.; Cheeseman, J. R.; Scalmani, G.; Barone, V.; Mennucci, B.; Petersson, G. A.; Nakatsuji, H.; Caricato, M.; Li, X.; Hratchian, H. P.; Izmaylov, A. F.; Bloino, J.; Zheng, G.; Sonnenberg, J. L.; Hada, M.; Ehara, M.; Toyota, K.; Fukuda, R.; Hasegawa, J.; Ishida, M.; Nakajima, T.; Honda, Y.; Kitao, O.; Nakai, H.; Vreven, T.; Montgomery, J. A., Jr.; Peralta, J. E.; Ogliaro, F.; Bearpark, M.; Heyd, J. J.; Brothers, E.; Kudin, K. N.; Staroverov, V. N.; Kobayashi, R.; Normand, J.; Raghavachari, K.; Rendell, A.; Burant, J. C.; Iyengar, S. S.; Tomasi, J.; Cossi, M.; Rega, N.; Millam, N. J.; Klene, M.; Knox, J. E.; Cross, J. B.; Bakken, V.; Adamo, C.; Jaramillo, J.; Gomperts, R.; Stratmann, R. E.; Yazyev, O.; Austin, A. J.; Cammi, R.; Pomelli, C.; Ochterski, J. W.; Martin, R. L.; Morokuma, K.; Zakrzewski, V. G.; Voth, G. A.; Salvador, P.; Dannenberg, J. J.; Dapprich, S.; Daniels, A. D.; Farkas, Ö.; Foresman, J. B.; Ortiz, J. V.; Cioslowski, J.; Fox, D. J.; *Gaussian 09, Rev A.02*; Gaussian, Inc.: Wallingford, CT, 2009.
73. Biegler-König, F.; Schönbohm, J.; Bayles, D.; *J. Comput. Chem.* **2001**, *22*, 545.
74. Jackson, P. L.; North, H.; Alexander, M. S.; Assey, G. E.; Scott, K. R.; Butcher, R. J.; *Acta Crystallogr., Sect. E: Struct. Rep. Online.* 2011, *67*, 2272.
75. Gutowsky, H. S.; McCall, D. W.; Slichter, C. P.; *Phys. Rev.* **1952**, *84***,** 589.
76. Blake, P. R.; Lee, B.; Summers, M. F.; Adams, M. W. W.; Park, J. B.; Zhou, Z. H.; Bax, A.; *J. Biomol. NMR*. **1992**, *2*, 527.
77. Blake, P. R.; Park, J. B.; Adams, M. W. W.; Summers, M. F.; *J. Am. Chem. Soc.* **1992**, *114*, 4931.
78. Bader, R. F. W.; Essén, H.; *J. Chem. Phys*. **1984**, *80*, 1943.
79. Espinosa, E.; Alkorta, I.; Elguero, J.; Molins, E.; *J. Chem. Phys*. **2002**, *117*, 5529.
80. Gibbs, G. V; Spackman, M. A.; Jayatilaka, D.; Rosso, K. M.; Cox, D. F.; Tech, V.; *J. Phys. Chem. A.* **2006**, *110*, 12259.
81. Matta, C. F.; Hernández-Trujillo, J.; Tang. T.; Bader, R. F. W.; *Chem. Eur. J.* **2003**, *9*, 1940.
82. Firme, C. L.; Pontes, D. D. L.; Antunes, O. A. C.; *Chem. Phys. Lett.* **2010**, *499*, 193.
83. Hernández-Trujillo, J.; Matta, C. F.; *Struct Chem.* **2007**, *18*, 849.
84. Mariam, Y. H.; Musin, R. N.; *J. Phys. Chem. A*. **2008**, *112*, 134.
85. Lapenda, T. L. S.; Morais, W. A.; Almeida, F. J. F.; Ferraz, M. S.; Lira, M. C. B.; Santos, N. P. S.; Maciel, M. A. M.; Santos-Magalhães, N. S.; *J. Biomed. Nanotechnol*. **2013**, *9*, 499.
86. Nascimento-Filho, J. M.; de Melo, C. P.; Santos-Magalhães, V. R.; Maciel, M. A. M.; Andrade, C. A. S.; *Colloids Surf., A*. **2010**, *358*, 42.
87. Canegim, B. H.; Serpeloni, J. M.; Maciel, M. A. M.; Cólus, I. M. S.; Mesquita, S. F. P.; *J. Med. Plants Res.* **2011**, *5*, 3277.
88. Lapenda, T. L. S.; Morais, W. A.; Lira, M. C. B.; Maciel, M. A. M.; Santos-Magalhães, N. S.; *Lat. Am. J. Pharm.* **2012**, *31*, 97.

Submitted: August 4, 2013
Published online: January 17, 2014